Influence of dual Ge/C pre-amorphization implantation on the Ni1–Pt Si phase nucleation and growth mechanisms

S. Guillemin, P. Gergaud, N. Bernier, L. Lachal, F. Mazen, A. Jannaud, F. Nemouchi, Ph. Rodriguez

Version of Record: https://www.sciencedirect.com/science/article/pii/S0167931721000733
Manuscript_de92796fa380e15c1f2bbeec1a67d1e2

Influence of dual Ge/C pre-amorphization implantation on the $Ni_{1-x}Pt_xSi$ phase nucleation and growth mechanisms

S. Guillemin[a,*], P. Gergaud[a], N. Bernier[a], L. Lachal[a], F. Mazen[a], A. Jannaud[a], F. Nemouchi[a], Ph. Rodriguez[a]

[a] *Univ. Grenoble Alpes, CEA, LETI, F-38000 Grenoble*

Abstract

The impact of dual Ge/C pre-amorphization implantation (PAI) processes on the $Ni_{0.9}Pt_{0.1}$(7nm)/Si system phase sequence has been investigated by advanced X-ray diffraction techniques and transmission electron microscopy (TEM). Using a high carbon implantation dose, it is found that the expected development of Ni-rich phases is not observed: a thick amorphous $Ni_{1-x}Pt_xSi$ layer developed until $Ni_{0.9}Pt_{0.1}$ full consumption, followed by the development of a thin crystalline $Ni_{1-x}Pt_xSi$ layer along the TiN interface. By increasing the temperature further, this last one abruptly thicken, creating the final silicide layer. An alternative model to grain boundary diffusion is discussed, accounting for the final distribution of the foreign species within the silicide layer. The use of Ge in dual Ge/C PAI is proposed to impact the growing mechanisms by alloying to fine-tune the carbon distribution in the substrate sub-surface.

Keywords: PAI, NiSi, silicides, solid-state-amorphization, SSA, impurity-enhanced solid-state-amorphization

1. Introduction

With the downscaling of CMOS technologies, the requirement of contact metallization schemes have become more and more demanding over the years.

*Corresponding author
Email address: sophie.guillemin@cea.fr (S. Guillemin)

With the rise of microtechnologies in the 1980s, together with the never-ending issue of lithography tool limitations, self-aligned silicide (salicide) processes appeared, C54-$TiSi_2$ being used as one of the first contact material. Silicides then quickly evolved to $CoSi_2$ and, finally, NiSi. Compared to C54-$TiSi_2$ and $CoSi_2$, along with other advantages, NiSi forms accordingly to diffusion limited mechanisms, which allow to lower the nucleation temperature and to obtain smoother interfaces [1]. The price to pay is a poor thermal stability and NiSi silicides are found not being able to withstand important thermal budgets. Two mechanisms are known to lead to NiSi layers degradation at high temperature: agglomeration and phase transition to higher resistive phase, the first one becoming dominant for thin films, where the relative importance of interfacial energy is strengthened [2]. To overcome this issue, several approaches inherited from previous silicide systems have been investigated, the use of alloying metals being the most widely spread one as of today. Among them, Pt shows an ability to postpone agglomeration without delaying NiSi nucleation or lowering the $NiSi_2$ nucleation temperature and is nowadays commonly implemented in the industry [3, 4]. The enhanced properties of silicides grown out of $Ni_{1-x}Pt_x$ metals layers are mainly explained by the poor solubility/low diffusion coefficient of Pt atoms in the growing phases, that leads to the stuffing of grain boundaries and NiSi/Si interface, and/or by the suppression of axiotaxial phenomena [5, 6]. To go even further, pre-amorphization implantation (PAI) processes, in which the deposition of the metal layer is preceded by an ion implantation step, have been subsequently studied. Compared to alloying, they further allow to modify the Si substrate crystallinity, providing this way an additional lever of controlling element diffusion, reactions at the silicide/silicon interface and/or nucleation processes. Within the optimized implantation conditions, Ge, C or dual Ge/C PAI processes have proven highly efficient in addressing the agglomeration problematic [7, 8, 9, 10, 11, 12]. Most strikingly, the use of carbon is delaying NiSi layers' agglomeration by several hundred of degrees Celsius, making of this specie one of the most promising ever reported. While introducing carbon in the substrate is expected to bring additional beneficial effects on de-

vices (such as a better control of dopant diffusion and induced tensile strain), it can also lead to an unacceptable increase of the silicide resistivity. On the other hand, Ge PAI processes, which have shown to have a less drastic effect on agglomeration, have proven particularly efficient at reducing the NiSi/Si interface roughness without being detrimental to the layers' resistivity. As a consequence, it has been proposed that dual Ge/C PAI processes would allow to combine the strong points of both species, without having to use too much carbon since the first Ge shot will bring the system close to, or even at, amorphization [13, 14]. Despite the good results obtained exploiting this idea, the literature regarding the underlying mechanisms is surprisingly scarce. Most typically, the formation mechanisms of the final silicide layer as well as the respective role of the first Ge shot with respect to the second C one regarding these mechanisms are still under debate. It is so the aim of this paper to cast a new light on these topics by proposing an in-depth study of four types of samples prepared using "progressive" implantation conditions, *i.e.* starting with a single Ge implantation PAI process and bringing more and more C into the system by adding a C implantation shot using an increasing dose.

2. Experimental

A series of four samples solely distinguished by the used pre-amorphization implantation conditions was prepared, using Si(100) bulk substrates as starting material. The ion implantation processes were all performed on a VIISTA HCP implanter from Applied Materials. Crystal TRansport of Ions in Matter (CTRIM) [15] simulations were first realized in order to determine the various energies and doses required for reaching full amorphization of the substrate, together with making sure that the created amorphous region is shallow enough so that it will be subsequently fully consumed by the silicidation process. One of the sample was not implanted, in order to serve as reference. For all the implanted samples, a first Ge shot at 5 keV using a dose of 1.10^{14} at.cm^{-2} was performed, which is expected to bring the system to its amorphous state over a

thickness around 7 nm, accordingly to our CTRIM simulations. For two of the three as prepared samples, a second implantation shot at 2 keV followed, using an increasing carbon dose of respectively 2.10^{15} at.cm^{-2} and 4.10^{15} at.cm^{-2}.

The four samples were then cleaned using a HF 0.5% solution and immediately carried away into an Endura 300 mm integrated platform from Applied Materials. This specific platform is equipped with several plugged modules, allowing to create integrated multi-step process sequences without air break. In the present study, the samples were first dry-cleaned using a NF_3/NH_4 based chemical etch (Siconi^{TM} process) in order to remove the native oxide layer that might have regrown during the transport. They were then moved through the magnetron sputtering deposition chambers, where the sequential deposition of a 7 nm thick $Ni_{0.9}Pt_{0.1}$ thin film and a 7 nm thick TiN capping layer was performed at room temperature.

The phase formation sequence and crystalline evolution of the $Ni_{0.9}Pt_{0.1}$/Si systems were monitored by in-situ X-ray diffraction (XRD) using an Empyrean PANalytical X-ray diffractometer equipped with a copper (Cu Kα) source, a linear detector (PIXcel1D) and a DHS1100 Anton Paar furnace under secondary vacuum (pressure was maintained below 10^{-4} bar to avoid atmospheric contamination). θ-2θ scans were performed with a 2° offset in ω in order to attenuate the symmetric (400) substrate reflection. Analyses were carried out from room temperature to 500 °C, with 5 °C steps and a scanning time of 7 min per temperature step. Phase analysis was performed with the HighScore Plus software from PANalytical (Degen *et al.*, 2014) and the ICDD PDF-4 database (http://www.icdd.com/). The results will be presented in the following over the 40° to 58° angular range in θ, which has been identified as the zone of interest in this study, *i.e.* no additional information regarding the sample texture evolution was found outside these borders. Complementary in-plane reciprocal space map (RSM) characterizations were carried out using a Rigaku SmartLab X-ray diffractometer. The grazing-incident angle was fixed at 0.5° and the exit angle for detection at 1°. The RSMs were obtained using an in-plane 2θ range of 20° to 80°, for a ϕ range of 100°, respectively explored with steps of 0.3° and

0.5°.

Lamellae for the TEM analysis were prepared by TripodTM polishing [16]. High-resolution STEM (HRSTEM) images were acquired on a ThermoFisher probe corrected Titan Themis microscope operated at 200 kV using a high-angle annular dark field (HAADF) detector. Nanobeam electron diffraction (NBED) patterns were acquired on a Gatan US1000 CCD camera after inserting a 10 μm C2 aperture to lower the convergence angle. EDX spectra were acquired on the same microscope using the super-X windowless detection system allowing for a solid angle of $\backsim$ 0.7 srad. Precession electron diffraction (PED) patterns were acquired on a ThermoFisher Tecnai Osiris microscope operated at 200 kV and equipped with the NanoMEGAS ASTAR system [17]. The microscope was set to microprobe mode with a 30 μm C2 aperture. The indexation of PED patterns in ASTAR software was performed using the CIF file 1532040 for the NiSi phase.

3. Results

The evolution of the $Ni_{0.9}Pt_{0.1}$/Si system phase sequence with the use of PAI processes as described in the experimental section is presented in Fig. 1. For the reference sample (Fig. 1(a)), the reaction starts with the consumption of the $Ni_{0.9}Pt_{0.1}$ layer by metal diffusion into the substrate, as shown by the progressive intensity decrease of the peak located around 43.8°. This peak corresponds to the Ni(111) diffraction line, with a slight down-shifting of 0.7° compared to PDF file 00-004-0850, that is mainly explained by the presence of Pt in the layer. The line intensity decrease is slow at first for then being progressively accelerated with the rise of the annealing temperature. Before full consumption of the layer around 190 °C, the diffraction peak starts shifting toward lowest angles, undergoing a total shift of about 1.1° at 185 °C, where the line is vanishing (see Fig. 2). This phenomenon, known as the snowplow effect in the literature, is the signature of the Pt atoms being expelled from the growing phase into the remaining metal layer, either because of their low solubility and/or their low

diffusion coefficient in this last one as compared to Ni atoms [18]. After full consumption of the $Ni_{0.9}Pt_{0.1}$ reservoir, two new diffraction lines measured at 54.6° and 55.9° are appearing around 270 °C, that respectively corresponds to the NiSi(020) and NiSi(013) diffraction planes. Similarly to what was observed for the as-deposited $Ni_{0.9}Pt_{0.1}$ layer, these peaks are measured at slightly lower angles than expected from PDF file 00-004-0850 by 0.5°. In this specific case, the origin of such a discrepancy is less straightforward since it is most likely the combination of various factors such as the lattice thermal expansion, the possible build-in of strain/stress constraints in the film during the silicide growth process and the incorporation of Pt within the growing phase. While it has been shown that stress/strain effects could have a strong impact on the development of silicide thin films, it is also expected that the layers would need to relax for the NiSi phase to nucleate and/or growth [19, 20, 21]. Regarding thermal expansion, it is known for years that NiSi present a strong anisotropy, its thermal expansion coefficient turning even negative along the b axis [22]. Since part of the grains composing the currently under discussion $Ni_{1-x}Pt_xSi$ layer are aligned along this axis (NiSi(020) line in Fig. 1), the observed line down-shifting is most likely not accounted for, or at least not solely accounted for, thermal expansion. In the light of these elements, it is subsequently proposed that some of the Pt atoms present in the $Ni_{0.9}Pt_{0.1}$ metal layer in its initial state are able to diffuse into the growing layer where they will be incorporated in the lattice, their amount being reduced compared to the initial 10% by the snowplow effect and possible stuffing of grain boundaries [20, 23]. After nucleation of the $Ni_{1-x}Pt_xSi$ phase around 270 °C, the system is not observed to significantly evolve up to 500 °C. It has to be noted that, in addition to the lines discussed up to this point, two faint diffraction lines respectively measured at 45.4° and 46.6° in Fig. 1(a) are present over the whole range of investigated temperatures. Passed 270 °C, they are proposed to be the signature of a $Ni_{1-x}Pt_xSi$ minority grain population, that would be randomly oriented. Below 270 °C, they are more difficult to be accounted for with certainty. Regarding the literature, several scenario are possible when considering NiSi sytems which are not showing

any intense diffraction lines after $Ni_{1-x}Pt_x$ full consumption. Typically, the diffusion of the metal layer into the substrate could be concomitant either with the development of a Ni-rich θ-Ni_2Si phase in epitaxy with the substrate or with the development of an amorphous NiSi layer [24, 25]. In the present case, since at least the line measured at 46.6° is observed from 50 °C on, the evolution of the system with the temperature is expected to be strongly influenced by the composition and/or texture of the intermixed layer grown on silicon during the $Ni_{0.9}Pt_{0.1}$ deposition process itself [26, 27, 20, 28]. As a consequence, an in-depth understanding of the phase sequence of our reference system below 270 °C would require additional data, which is not the object of the present work and will be addressed in a following paper.

Within the chosen implantation conditions, the introduction of Ge atoms in the Si substrate near-surface area is not shown to have any substantial measurable effects on the $Ni_{0.9}Pt_{0.1}$/Si system phase sequence (Fig. 1(b)). On the contrary, adding additional C atoms in the equation by the means of a sequential second implantation shot modify the NiSi layer final texture by strengthening its orientation along the [020] and [013] axis and strongly impacts the NiSi phase nucleation temperature: $Ni_{1-x}Pt_xSi$ is found to nucleate at 315 °C (respectively 440 °C) for low (respectively high) C implantation doses, *i.e.* 45 °C (respectively 170 °C) latter than the 270 °C obtained for the reference sample (see Fig. 1(c) and Fig. 1(d)). For the highest C dose of 4.10^{15} at.cm^{-2}, even the diffusion kinetics are modified since the $Ni_{0.9}Pt_{0.1}$ layer full consumption is slightly postponed from 190 °C to 215 °C. Additionally, by plotting the position of the $Ni_{0.9}Pt_{0.1}$ peak with the annealing temperature in Fig. 2, it is revealed that the snowplow effect is almost fully suppressed for this very same sample. In order to gain understanding on the fundamental mechanisms behind the striking results describe hereinabove, additional analyses have thus been performed on the sample where a high carbon implantation dose has been used.

First, the texture of the grown $Ni_{1-x}Pt_xSi$ layer after in-situ annealing up to 500 °C and following cool-down to room temperature was characterized by in-plane RSM measurement. The corresponding 3D contour map is presented

in Fig. 3(a) and shows a series of lines that is characteristic of a fiber texture. Once indexed, and using CaRIne 3.1 software, it is confirmed that those lines correspond to a layer composed of grains aligned either along the NiSi[020] or the NiSi[013] direction. The corresponding pattern integrated over the whole ϕ angular range is presented in Fig. 3(b), together with the one obtained for the reference sample using the same procedure. It is shown that, except for some line intensity variations related to the higher degree of texture in the dual implanted sample, the addition of carbon in the $Ni_{0.9}Pt_{0.1}$/Si system is not drastically impacting its final texture state. Additionally, through this integration method, it is possible 1) to extract the angular shifts of the various diffraction lines with respect to the diffraction angles reported in PDF files and 2) to perform a comparative analysis over the samples of the peaks' full width at half maximum (FWHM) which is to be inversely related to the in-plane crystallite average diameter in thin silicide films assuming that no extended structural defects are expected to develop during the growth. While the first operation is straightforward, the second one is more delicate and only the lines with enough intensity and no dual contribution have to be considered, *i.e.* NiSi(002), NiSi(102) and NiSi(202) when comparing the currently under discussion implanted sample to the reference. The results are presented in Fig. 3(c) and 3(d), respectively. On the one hand, it is shown that the lines' shift is more pronounced when using the dual Ge/C PAI process with a high carbon dose of 4.10^{15} at.cm^{-2} than for the reference sample. The amount of Ge atoms brought into the system by implantation, that is about 0.27% of the Si contribution, is considered too low to have any measurable effect on the lattice parameters. It is thus concluded that either the presence of carbon in the system is allowing the incorporation of more Pt in the final $Ni_{1-x}Pt_xSi$ lattice or the carbon itself is incorporated in the lattice, as interstitial. On the other hand, the FWHM of the NiSi(002), NiSi(102) and NiSi(202) diffraction peaks is larger for the C-implanted sample as compared to reference. While it should be further confirmed on the whole set available of diffraction lines, which would imply a much longer counting time due to experimental limitations, it is accordingly expected that the average grain diameter

of $Ni_{1-x}Pt_xSi$ layers obtained using C-based PAI processes will be smaller.

Second, the intermediate stages of the solid-state reaction between the $Ni_{0.9}Pt_{0.1}$ metal layer and the dual Ge(5 keV, 1.10^{14} at.cm^{-2})/C(2 keV, 4.10^{15} at.cm^{-2}) implanted Si substrate have been investigated through the realization of quenched samples at 240 °C, 280 °C and 360 °C. The same annealing ramp as the one used for in-situ XRD analysis was used, after what the samples were cooled down to room temperature and analysed by in-plane RSM. The corresponding integrated patterns are presented in Fig. 4. For all the investigated quenched temperatures, the obtained set of diffraction lines can solely be attributed to the $Ni_{1-x}Pt_xSi$ phase. At 240 °C and 280 °C, only the most intense lines are visible and the corresponding peaks are characterized by a very broad FWHM, meaning that the layer is close to an amorphous state. With increasing the quench's temperature, the peaks' FWHM is observed to decrease quite strongly, implying that the average diameter of the crystallites composing the layer is increasing, reaching its final value between 360 °C and 500 °C.

Finally, two TEM lamellae were prepared, one out of the sample quenched at 360 °C (see Fig. 5) and one out of the sample annealed up to 500 °C (see Fig. 6). From the quenched sample, it is revealed in Fig. 5(a) that the system is composed of a thick amorphous layer and a thin, almost continuous crystalline layer on top, at the interface with the TiN capping layer. This is confirmed by NBED patterns, respectively taken from one and the other of these two distinct area, as seen in insert in Fig. 5(a), and by PED analysis, as seen in Fig. 5(b). The $Ni_{1-x}Pt_x$:Si ratio is close to 1:1 through the whole $Ni_{1-x}Pt_xSi$ layer, with the Pt to Ni ratio increased in the crystalline top layer as compared to its amorphous counterpart (see energy-dispersive X-ray spectroscopy (EDXS) results, Fig. 5(c)). A small amount of Pt is found at the interface with Si, which is most probably the consequence of some of the Pt atoms being caught by the moving a-$Ni_{1-x}Pt_xSi$ interface during annealing. After annealing at 500 °C, it is shown in Fig. 6(a) that a continuous 14 nm thick c-$Ni_{1-x}Pt_xSi$ is obtained, presenting a low interface roughness with Si. The underlying substrate is found to be slightly damaged by the used PAI process. Coherently to XRD results, it

is confirmed by ASTAR mappings Fig. 6(b) that the $Ni_{1-x}Pt_xSi$ layer is composed of small grains that are either aligned along the [020] or [013] direction. Compared to the intermediate state (sample quenched at 360 °C), Pt atoms are more evenly distributed, nevertheless keeping the initial profile shape. This phenomena is to be attributed to the Pt diffusion within the layer accordingly to its compositional gradient, confirming its miscibility in the medium and supporting the hypothesis that the XRD shift observed in Fig. 3(c) is to be attributed to Pt atoms incorporated in the lattice. It exists an apparent discrepancy in-between the results obtained through in-situ XRD analysis and the one obtained through in-plane RSM and TEM analysis: while NiSi diffraction lines were only observed from 440 °C on in Fig. 1, peaks corresponding to this compound are already present at 240 °C in Fig. 4 and a thin NiSi layer is observed by TEM imaging at 360 °C in Fig. 5. This is explained by the limited sensitivity of in-situ XRD procedures where each acquisition is taking only a few minutes, meaning that the layer needs to thicken for making the XRD signal possible to detect in this specific configuration.

4. Discussion

The sequential transition from a fully grown a-NiSi layer to a c-NiSi silicide has recently been reported in other NiSi systems modified through the incorporation of impurities. Typically, K. van Stiphout *et al.* have proposed a detailed discussion on the impact of impurities-enhanced solid-sate amorphization (SSA) processes, which describes the development of an amorphous layer upon annealing [29, 30]. The development of such a layer at low temperature can be related to the incapability of crystalline phases to nucleate due to nucleation barrier effects and/or to growth instability mechanisms where the phase having the best potential of lowering the Gibb´s free energy will suppress the development of any other phase until its growth is sufficiently slowed down. Nucleation barriers can themselves be related either to kinetics effects (*i.e.* the energy required for the atoms to rearrange themselves) or to thermodynamic ones (*i.e.* the energy

required to overcome the creation of a new interface), that are respectively expected to be dominant at low or high temperature. In this context, K. van Stiphout *et al.* proposed that the introduction of N atoms in Ni/Si systems is promoting the growth of a thick amorphous NiSi layer by raising the kinetic nucleation barriers due to 1) the insolubility of nitrogen in any stable, crystalline Ni silicide and 2) the ability of nitrogen to strongly bind itself with Si, making it difficult to expel from the NiSi phase to grow.

Since the chemical properties of carbon are close to the ones of nitrogen, the full conversion under annealing of a 7 nm $Ni_{0.9}Pt_{0.1}$ layer into an amorphous $Ni_{1-x}Pt_xSi$, that is observed in the present work when using a C-based PAI process, is proposed to obey the same mechanisms. Consequently, C atoms, once expelled from the growing phase, are expected to segregate at grains boundaries and the $Ni_{1-x}Pt_xSi$ peak shift observed in Fig. 3, as compared to the reference sample, is most probably to be related to the incorporation of more Pt in the lattice, as substitutional atoms. More interestingly, the additional findings described in this paper allow to move the discussion forward, by considering the impact of adding carbon into the $Ni_{0.9}Pt_{0.1}$/Si system on the nucleation and growth kinetics of the $Ni_{1-x}Pt_xSi$ phase itself. Putting in perspective the results obtained through XRD analysis and TEM imaging, two scenarios can be envisioned. The first one is based on classical phase sequential growth theories, stating that the crystalline NiSi phase would nucleate from an intermediate grown phase in the form of small nucleus that would then grow laterally until forming a continuous layer [20, 5, 21]. From there on, it is further expected that the layer will abruptly thicken to form the final silicide layer. In the present case, this model would imply that the $Ni_{1-x}Pt_xSi$ phase is actually nucleating in a sequential manner out of the amorphous $Ni_{1-x}Pt_xSi$ phase at low temperature (*i.e.* inferior to 240 °C) and that the presence of C in the system would strongly hampers the NiSi nuclei lateral growth, postponing the formation of a continuous layer to more than 360 °C. It is quite surprising that the crystalline layer should nucleate at the TiN interface rather than at the interface with Si, but two important factors must be discussed in this regard. First, stress effects

are expected to be high in the upper area of the grown a-NiSi layer, due to the presence of the TiN capping layer: using our process of reference (POR), a compressive layer with no less than -5.8 GPa is obtained. As a consequence, the nucleation of the c-$Ni_{1-x}Pt_xSi$ layer at the interface with TiN could be related to the system attempt to minimize its interfacial energy. Additionally, since the crystalline layer observed in Fig. 5 corresponds to a Pt-rich area, it is further possible that the nucleation of crystalline nuclei at the interface with TiN might be facilitated by lattice distortion effects. The second scenario considers the possible strengthened role in our system of the Ni/Si intermixed layer, which is expected to form during the $Ni_{0.9}Pt_{0.1}$ deposition process at the interface with Si, as a consequence of the energy brought to the system by the PVD process [31, 20]. Since the thickness of the crystalline layer observed by TEM imaging at 360 °C is consistent with the one expected for such an intermixed layer, it could be the case that this layer is nanocrystalline from the start, and that the sharpening of the $Ni_{1-x}Pt_xSi$ peaks observed in Fig. 4 would be the signature of coalescence events. In this second scenario, the $Ni_{1-x}Pt_xSi$ would nucleate at the c-$Ni_{1-x}Pt_xSi$/a-$Ni_{1-x}Pt_xSi$ interface at rather high temperature (*i.e.* superior to 360 °C), for then abruptly thicken. In both scenarios, the thickening of the $Ni_{1-x}Pt_xSi$ is driven by diffusion processes, explaining the smooth interface with Si observed in Fig. 6. Similarly, both scenarios are expected to lead to a layer composed of small grains since the presence of C is straightening the competition between nucleation rate and nuclei lateral growth.

Importantly, the diffusion kinetic of foreign species brought into the Ni/Si system by metal alloying (Pt) and PAI processes (Ge) is additionally expected to be modified in the presence of carbon atoms. Maybe even more important, the mechanisms involved in the diffusion phenomena themselves are going to differ from the regular case of the sequential growth of crystalline $Ni_{1-x}Si_x$ phases. Typically, the distribution of a foreign species in a system is driven by several factors including: 1) its solubility in the present phases, which fixes the maximum amount of the considered foreign atoms that can be incorporated in the lattice 2) its diffusion coefficient that could limit its incorporation in the

growing layer 3) segregation, which is the movement of foreign atoms towards surface/interfaces of high energies in order to stabilize them and 4) stress relaxation, meaning that some atoms might been pushed to move toward interfaces in order to relax the system [20, 32]. In all cases, the diffusion through GBs will widely be favoured over bulk diffusion, due to much higher diffusion coefficient in these area. In the system under investigation, the presence of carbon favours the development and stabilization of a thick amorphous layer, *i.e.* a layer exempt of GBs. In this respect, the less pronounced Pt snowplow effect observed for the Ge/C dual implanted sample where the consumption of the metal layer is postponed to 215 °C gives direct proof that it is the low diffusion coefficient of Pt in the a-$Ni_{1-x}Pt_xSi$ layer (as compared to the one of Ni), rather than the limited solubility of this element in a-$Ni_{1-x}Pt_xSi$ media, that limits the incorporation of Pt. It further suggests that the incorporation of carbon in a-Si phases is unevenly affecting Pt and Ni diffusion. Whether this trend is to be linked to different bulk diffusion mechanisms or to the very chemical nature of elements cannot be disentangle here and would require further investigation. Regarding Ge atoms, which have been considered as relevant tracers in Ni/Si systems due to their chemical properties and total miscibility in all $Ni_{1-x}Si_x$ phases [32], diffusion movements are mainly expected to be happening through segregation. In the presence of carbon atoms, which are expecting to be expelled from the c-$Ni_{1-x}Pt_xSi$ phase for this last one to develop, the minimization of surface and interface energies is expected to be ensured by C segregation. The distribution of Ge atoms will so not differ strongly from the one obtained after implantation, as was shown in a previous report [33].

In the light of the presented results and following discussion, it would seem that the impact of Ge atoms brought by PAI processes on the $Ni_{0.9}Pt_{0.1}$/Si system phase sequence and associated diffusion mechanisms is overruled by C effects for dual Ge/C implantation procedures. Nevertheless, additional measurements (not shown here) have proven that performing a single C implantation shot at 2 keV using a dose of 4.10^{15} at.cm^{-2} is less efficient at postponing the formation of a continuous c-$Ni_{1-x}Pt_xSi$ layer than dual Ge/C PAI processes us-

ing the same C implantation conditions. Once again, this can be understood by making some parallels with the development of thick a-NiSi layers by impurities-enhanced SSA processes. Typically, K. van Stiphout *et al.* have shown that the localization of N atoms in their system appear to be a critical parameter in order for SSA to proceed, meaning that it is the amount of foreign species at the growing interface that has to be sufficient for the process to take place [29]. This hypothesis is supported by De Keyser *et al.* that showed that only the introduction of an inter-layer of C atoms can suppress the Ni-rich phases from the Ni/Si phase sequence compared to $Si_{1-x}C_x$ substrates or alloyed layers [34]. In this regard, it can be proposed that the first Ge shot can be used as a lever to tune the C distribution in the layer. This would have several beneficial effects on adjusting the trade-off between layer resistivity and degradation at high temperature including limiting the decrease of the average grain size and inducing a more homogeneous incorporation of the Pt atoms in the final layer (*i.e.* postponing the transition to $Ni_{1-x}Pt_xSi_2$).

5. Conclusion

While previous reports from the literature have shown the great potential of carbon-based PAI processes at postponing NiSi agglomeration at high temperature, the present study focus on the formation mechanisms of the NiSi phase when using such processes. In order to get as close as possible to industrial roadmaps, $Ni_{0.9}Pt_{0.1}$ alloy layers were used as metal material, adding a degree of complexity in the system since the Pt atoms will act as an additional foreign species. Similarly to what has been observed for N-implanted silicon substrates, the silicidation process shows an alternative phase sequence as compared to the classical sequential/transient growth of Ni-rich phases: for the last sample of the studied series (Ge/C dual implantation process, 4.10^{15} at.cm^{-2} used for the carbon implantation shot), a thick amorphous $Ni_{1-x}Pt_xSi$ layer developed until $Ni_{0.9}Pt_{0.1}$ full consumption, from which the c-$Ni_{1-x}Pt_xSi$ nucleates. From there on, the crystallization process is strongly hampered by the presence of carbon,

which needs to be expelled from the growing phase for this last one to develop. This explains the strong temperature delay observed in the appearance of NiSi diffraction lines when annealing the samples under X-ray diffraction, which is observed to be proportional to the amount of carbon present in the system. Additionally, using in this study progressive PAI implantation conditions along the samples has allowed to disentangle the effects induced by the presence of Ge atoms, on the one side, and C atoms, on the other side, on the system evolution. It is found that, despite the fact that only carbon is observed to impact the system phase sequence in a substantial way, the use of dual Ge/C processes is beneficial since it should allow to control the carbon implantation profile. Finally, the growth mechanisms described in this paper are shown to strongly impact the diffusion mechanisms of foreign species in the system as compared to classical Ni-rich sequential/transient phase sequences. This is explained by the absence of grain boundaries during most of the layer development, hampering the foreign species movements. It has to be noted that the results presented in this paper are paving the way for additional studies. Typically, the role of stress/strain in the c-$Ni_{1-x}Pt_xSi$ nucleation mechanisms is still to be clarified. Also, while the current study has allowed to gain understanding of the various available levels to tune the properties of silicide layers, it has also enlightened the need of making compromises. In particular, using carbon to postpone NiSi agglomeration at high temperature would also postpone the full development of this same layer at low temperature. As such, any additional work aiming at tunning the experimental conditions should be correlated to devices specifications.

6. Acknowledgements

This research was supported by the French National Research Agency (ANR) under the "Investissements d'avenir" program ANR 10-EQPX-0030 (EQUIPEX FDSOI 11) and by the Nano2022 project. It also received additional funding from the ECSEL Joint Undertaking (JU) under grant agreement No 783127.

The JU receives support from the European Union's Horizon 2020 research and innovation programme and France, Germany, Austria, Portugal, Greece, Spain, Poland.

References

[1] C. Lavoie, F. M. d´Heurle, S.-L. Zhang, Handbook of Semiconductor Manufacturing Technology Chapter 10, CRC Press, 2017.

[2] D. Deduytsche, C. Detavernier, R. L. Van Meirhaeghe, C. Lavoie, High-temperature degradation of NiSi films: Agglomeration versus $NiSi_2$ nucleation, Journal of Applied Physics 98 (3) (2005) 033526. doi:10.1063/1.2005380.

[3] D. Mangelinck, J. Y. Dai, J. S. Pan, S. K. Lahiri, Enhancement of thermal stability of NiSi films on (100)Si and (111)Si by Pt addition, Applied Physics Letters 75 (12) (1999) 1736–1738. doi:10.1063/1.124803.

[4] C. Lavoie, C. Detavernier, C. Cabral, F. d'Heurle, A. Kellock, J. Jordan-Sweet, J. Harper, Effects of additive elements on the phase formation and morphological stability of nickel monosilicide films, Microelectronic Engineering 83 (11) (2006) 2042–2054. doi:10.1016/j.mee.2006.09.006.

[5] J. Demeulemeester, D. Smeets, C. M. Comrie, N. P. Barradas, A. Vieira, C. Van Bockstael, C. Detavernier, K. Temst, A. Vantomme, On the growth kinetics of Ni(Pt) silicide thin films, Journal of Applied Physics 113 (16) (2013) 163504. doi:10.1063/1.4802738.

[6] C. Detavernier, C. Lavoie, Influence of Pt addition on the texture of NiSi on Si(001), Applied Physics Letters 84 (18) (2004) 3549–3551. doi:10.1063/1.1719276.

[7] B.-Y. Tsui, C.-M. Hsieh, Y.-R. Hung, Y. Yang, R. Shen, S. Cheng, T. Lin, Improvement of the Thermal Stability of NiSi by Germanium Ion Implan-

tation, Journal of The Electrochemical Society 157 (2) (2010) H137–H143. doi:10.1149/1.3261852.

[8] O. Nakatsuka, K. Okubo, A. Sakai, M. Ogawa, Y. Yasuda, S. Zaima, Improvement in NiSi/Si contact properties with C-implantation, Microelectronic Engineering 82 (3) (2005) 479–484, Proceedings of the ninth european workshop on materials for advanced metallization 2005. doi:10.1016/j.mee.2005.07.046.

[9] S. Mertens, T. Y. Hoffmann, C. Vrancken, S. Jakschik, O. Richard, E. Verleysen, H. Bender, C. Zhao, W. Vandervorst, P. Absil, A. Lauwers, NI (PT) SI Thermal Stability Improvement by Carbon Implantation, in: ECS Transactions, ECS, 2008. doi:10.1149/1.2911522.

[10] A. S. Ozcan, D. Wall, J. Jordan-Sweet, C. Lavoie, Effects of temperature dependent pre-amorphization implantation on NiPt silicide formation and thermal stability on Si(100), Applied Physics Letters 102 (17) (2013) 172107. doi:10.1063/1.4801928.

[11] J. Luo, Z.-J. Qiu, J. Deng, C. Zhao, J. Li, W. Wang, D. Chen, D. Wu, M. Östling, T. Ye, S.-L. Zhang, Effects of carbon pre-silicidation implant into Si substrate on NiSi, Microelectronic Engineering 120 (2014) 178–181, MAM2013, March 10-13, Leuven, Belgium. doi:10.1016/j.mee.2013.08.010.

[12] L. Lachal, P. Rodriguez, M. Grégoire, E. Ghegin, F. Milesi, M. Coig, J. Borrel, S. Joblot, M. Juhel, F. Nemouchi, F. Mazen, Effects of Pre-amorphization Thickness and Carbon Implantation on NiPt/Si Silicidation Process, in: 2018 22nd International Conference on Ion Implantation Technology (IIT), 2018, pp. 54–57. doi:10.1109/IIT.2018.8807963.

[13] C. Ortolland, M. Togo, E. Rosseel, S. Mertens, J. Kittl, P. Absil, A. Lauwers, T. Hoffmann, New carbon-based thermal stability improvement technique for NiPtSi used in CMOS technology, Microelectronic Engineering 88 (5) (2011) 578–582. doi:10.1016/j.mee.2010.07.008.

[14] T. Schram, A. Spessot, R. Ritzenthaler, E. Rosseel, C. Caillat, N. Horiguchi, Ni(Pt) silicide with improved thermal stability for application in DRAM periphery and replacement metal gate devices, Microelectronic Engineering 120 (2014) 157–162, MAM2013, March 10-13, Leuven, Belgium. doi:10.1016/j.mee.2013.12.012.

[15] M. Posselt, J. Biersack, Computer simulation of ion implantation into crystalline targets, Nuclear Instruments and Methods in Physics Research Section B: Beam Interactions with Materials and Atoms 64 (1) (1992) 706–710. doi:https://doi.org/10.1016/0168-583X(92)95562-6.

[16] J. P. Benedict, R. Anderson, S. J. Klepeis, M. Chaker, A Procedure for Cross Sectioning Specific Semiconductor Devices for Both SEM and TEM Analysis, MRS Proceedings 199 (1990) 189. doi:10.1557/PROC-199-189.

[17] E. F. Rauch, J. Portillo, S. Nicolopoulos, D. Bultreys, S. Rouvimov, P. Moeck, Automated nanocrystal orientation and phase mapping in the transmission electron microscope on the basis of precession electron diffraction, Zeitschrift für Kristallographie 225 (2-3) (2010) 103–109. doi:10.1524/zkri.2010.1205.

[18] O. Cojocaru-Mirédin, D. Mangelinck, K. Hoummada, E. Cadel, D. Blavette, B. Deconihout, C. Perrin-Pellegrino, Snowplow effect and reactive diffusion in the pt doped ni–si system, Scripta Materialia 57 (5) (2007) 373–376. doi:10.1016/j.scriptamat.2007.05.007.

[19] D. Mangelinck, K. Hoummada, Effect of stress on the transformation of Ni_2Si into NiSi, Applied Physics Letters 92 (25) (2008) 254101. doi:10.1063/1.2949751.

[20] K. Hoummada, C. Perrin-Pellegrino, D. Mangelinck, Effect of Pt addition on Ni silicide formation at low temperature: Growth, redistribution, and solubility, Journal of Applied Physics 106 (6) (2009) 063511. doi:10.1063/1.3204948.

[21] M. El Kousseifi, K. Hoummada, F. Panciera, C. Lavoie, D. Mangelinck, Nucleation and lateral growth kinetics of the NiSi phase at the epitaxial θ-Ni_2Si/Si interface, Acta Materialia 198 (2020) 100–110. doi:10.1016/j.actamat.2020.07.062.

[22] C. Detavernier, C. Lavoie, F. M. d'Heurle, Thermal expansion of the isostructural PtSi and NiSi: Negative expansion coefficient in NiSi and stress effects in thin films, Journal of Applied Physics 93 (5) (2003) 2510–2515. doi:10.1063/1.1545156.

[23] D. Mangelinck, K. Hoummada, A. Portavoce, C. Perrin, R. Daineche, M. Descoins, D. J. Larson, P. H. Clifton, Three-dimensional composition mapping of NiSi phase distribution and Pt diffusion via grain boundaries in Ni_2Si, Scripta Materialia 62 (8) (2010) 568–571. doi:10.1016/j.scriptamat.2009.12.044.

[24] F. Panciera, D. Mangelinck, K. Hoummada, M. Texier, M. Bertoglio, A. D. Luca, M. Gregoire, M. Juhela, Direct epitaxial growth of θ-Ni_2Si by reaction of a thin Ni(10 at.% Pt) film with Si(100) substrate, Scripta Materialia 78-79 (2014) 9–12. doi:10.1016/j.scriptamat.2014.01.010.

[25] J. Fouet, M. Texier, M.-I. Richard, A. Portavoce, D. Mangelinck, C. Guichet, N. Boudet, O. Thomas, Silicide formation during reaction between Ni ultra-thin films and Si(001) substrates, Materials Letters 116 (2014) 139–142. doi:10.1016/j.matlet.2013.10.119.

[26] S. Gaudet, C. Coia, P. Desjardins, C. Lavoie, Metastable phase formation during the reaction of Ni films with Si(001): The role of texture inheritance, Journal of Applied Physics 107 (9) (2010) 093515. doi:10.1063/1.3327451.

[27] S. Gaudet, P. Desjardins, C. Lavoie, The thermally-induced reaction of thin Ni films with Si: Effect of the substrate orientation, Journal of Applied Physics 110 (11) (2011) 113524. doi:10.1063/1.3662110.

[28] M. El Kousseifi, K. Hoummada, M. Bertoglio, D. Mangelinck, Selection of the first Ni silicide phase by controlling the Pt incorporation in the intermixed layer, Acta Materialia 106 (2016) 193–198. doi:10.1016/j.actamat.2016.01.004.

[29] K. van Stiphout, F. A. Geenen, N. M. Santos, S. M. C. Miranda, V. Joly, J. Demeulemeester, C. Detavernier, F. Kremer, L. M. C. Pereira, K. Temst, A. Vantomme, Impurity-enhanced solid-state amorphization: the Ni–Si thin film reaction altered by nitrogen, Journal of Physics D: Applied Physics 52 (14) (2019) 145301. doi:10.1088/1361-6463/ab00d2.

[30] K. van Stiphout, F. A. Geenen, N. M. Santos, S. M. C. Miranda, V. Joly, J. Demeulemeester, C. Mocuta, C. M. Comrie, C. Detavernier, L. M. C. Pereira, K. Temst, A. Vantomme, Ion beam modification of the Ni-Si solid-phase reaction: The influence of substrate damage and nitrogen impurities introduced by ion implantation, Journal of Physics D: Applied Physics 54 (1) (2020) 015307. doi:10.1088/1361-6463/abb046.

[31] K. Hoummada, E. Cadel, D. Mangelinck, C. Perrin-Pellegrino, D. Blavette, B. Deconihout, First stages of the formation of Ni silicide by atom probe tomography, Applied Physics Letters 89 (18) (2006) 181905. doi:10.1063/1.2370501.

[32] M. El Kousseifi, K. Hoummada, D. Mangelinck, Ni silicide study at the atomic scale: Diffusing species, relaxation and grooving mechanisms, Acta Materialia 83 (2015) 488–498. doi:10.1016/j.actamat.2014.10.029.

[33] P. Rodriguez, L. Lachal, M. Grégoire, E. Ghegin, R. Famulok, M. Lemang, J. Borrel, S. Joblot, M. Juhel, K. Dabertrand, F. Mazen, F. Nemouchi, Impact of Si and Ge pre-amorphization implantation on NiPt silicide properties, in: 2018 Materials for Advanced Metallization Conference, 2018.

[34] K. De Keyser, B. De Schutter, C. Detavernier, V. Machkaoutsan, M. Bauer, S. Thomas, J. Jordan Sweet, C. Lavoie, Phase formation and texture of

nickel silicides on $Si_{1-x}C_x$ epilayers, Microelectronic Engineering 88 (5) (2011) 536–540. doi:10.1016/j.mee.2010.06.010.

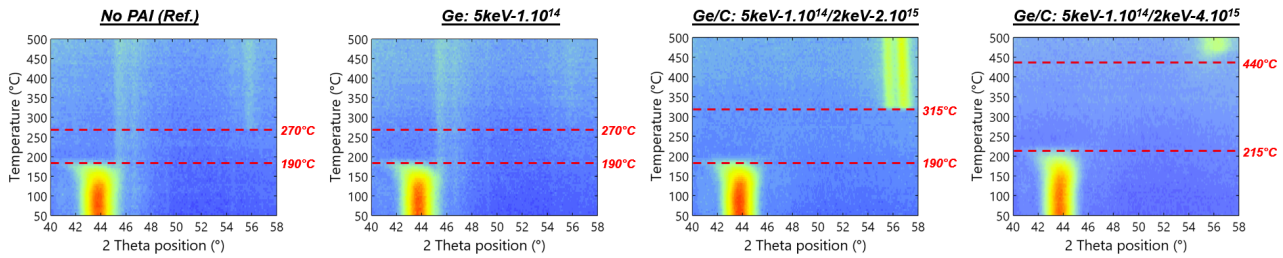

Figure 1: In-situ X-ray diffraction mappings corresponding to the reaction between a 7 nm $Ni_{0.9}Pt_{0.1}$ metal layer and the underlying Si substrate used in its as-grown state (a) or which has been implanted beforehand using a single Ge implantation shot at 5 keV / 1.10^{14} at.cm^{-2} (b) or a dual implantation process involving a first Ge shot at 5 keV / 1.10^{14} at.cm^{-2} followed by a second C shot either at 2 keV / 2.10^{15} at.cm^{-2} (c) or at 2 keV / 4.10^{15} at.cm^{-2} (d). The dashed red lines correspond to the temperature of metal full consumption and the temperature at which diffraction lines corresponding to the $Ni_{1-x}Pt_xSi$ compound appear, respectively.

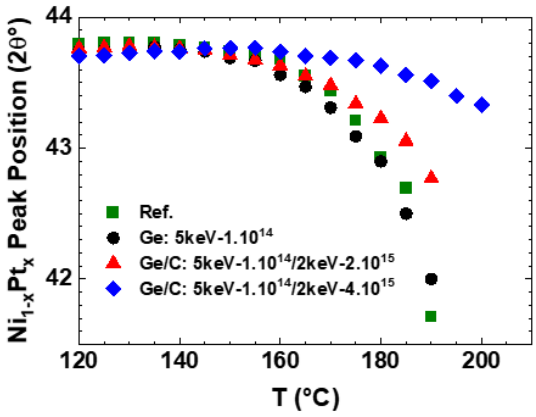

Figure 2: Evolution of the $Ni_{0.9}Pt_{0.1}(111)$ diffraction line position with the annealing temperature for the four systems studied by in-situ X-ray diffraction, as defined in Fig. 1.

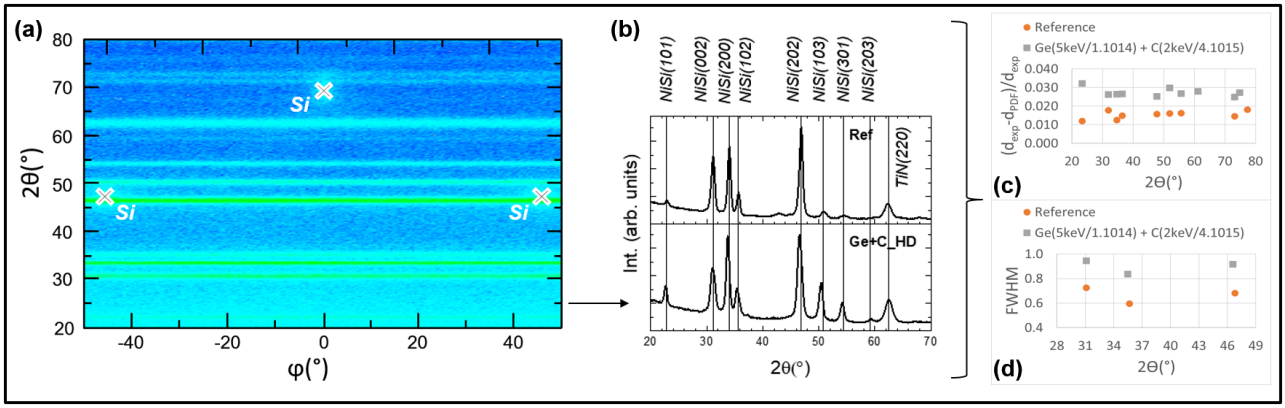

Figure 3: (a) In-plane reciprocal space map recorded after in-situ annealing up to 500 °C and subsequent cool-down to room temperature of the sample presented Fig. 1(d), *i.e.* where the Si substrate was implanted using a dual implantation process and a high carbon dose. (b) Integration of the data over the whole investigated ϕ range and comparison with the spectra obtained using the same procedure for the non-implanted Si substrate sample. (c) Corresponding extraction of the lines' shift, as compared to PDF file 00-004-0850. (d) Corresponding lines' full width at half maximum comparison, for the three relevant diffraction peaks (see discussion in main text).

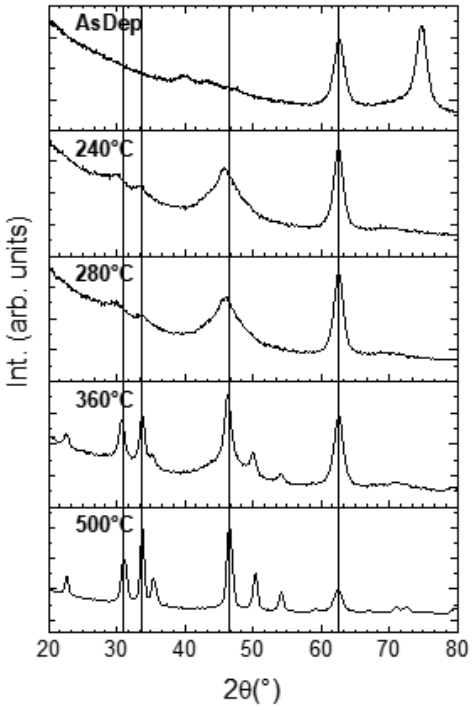

Figure 4: Diffraction diagrams obtained after integration over the whole investigated ϕ range (*i.e.* 100°) of in-plane reciprocal space map data. The samples were annealed using the same ramp as for in-situ X-ray diffraction analysis (see Fig. 1), stopping the annealing at various quenched temperatures and letting the system cool-down before starting the measurements. The whole series corresponds to samples where the Si substrate was modified using a dual implantation process involving a first Ge shot at 5 keV / 1.10^{14} at.cm^{-2} followed by a second C shot at 2 keV / 4.10^{15} at.m^{-2} before $Ni_{0.9}Pt_{0.1}$ metal deposition and subsequent silicidation.

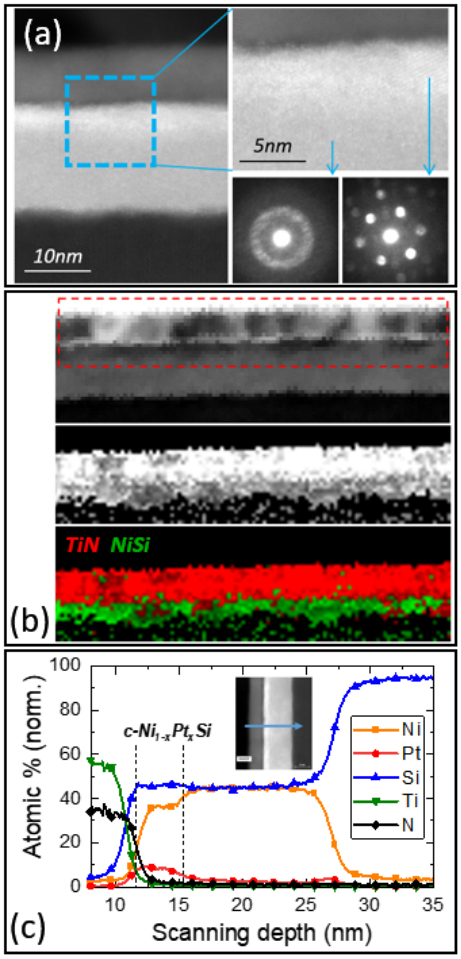

Figure 5: TEM results corresponding to the 7 nm thick $Ni_{0.9}Pt_{0.1}$ layer deposited on top of a dual Ge/C implanted Si sample (see text) after annealing under in-situ X-ray radiation up to 360 °C. (a) HRSTEM images of the stack with a magnified image on the crystalline $Ni_{1-x}Pt_xSi$ layer located under the TiN layer (in inset, local NBED patterns taken from the crystalline and amorphous zones). (b) Top: overview image - PED analysis performed within the dotted red rectangle; center: index image related to the quality of the indexation process, dark pixels corresponding to amorphous zones; bottom: phase map showing the indexation results using the TiN (in red) and NiSi (in green) structures. (c) Composition profile across the stack measured by EDX.

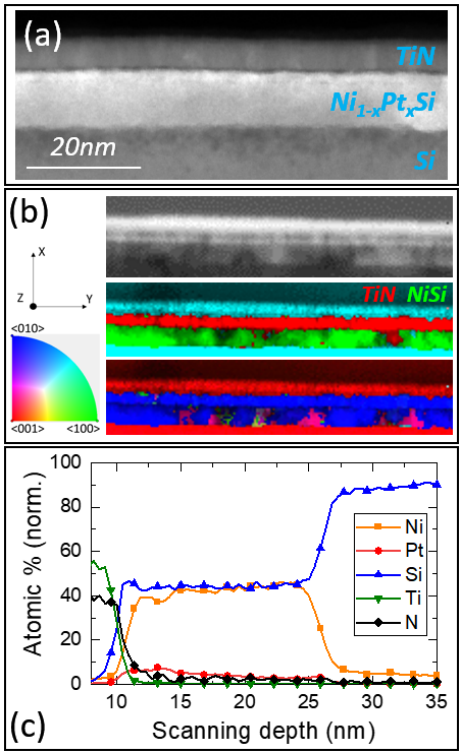

Figure 6: TEM results corresponding to the 7 nm thick $Ni_{0.9}Pt_{0.1}$ layer deposited on top of a dual Ge/C implanted Si sample (see text) after annealing under in-situ X-ray radiation up to 500 °C. (a) HRSTEM image of the stack. (b) Top: overview image for the PED analysis; center: phase map showing the indexation results using the TiN (in red) and NiSi (in green) structures; bottom: inverse pole figure (IPF) mapping along the X direction, showing that the $Ni_{1-x}Pt_xSi$ layer exhibits one main $\langle 010 \rangle$ orientation along the X growth direction with few grains (marked in purple) for which the $\langle 013 \rangle$ crystallographic direction is parallel to X. (c) Composition profile across the stack measured by EDX.